

Proceedings of the XV-th National School “Hundred Years of Superconductivity”, Kazimierz Dolny, October 9–13, 2011

Strong-Coupling Description of the High-Temperature Superconductivity in the Molecular Hydrogen

R. SZCZEŚNIAK AND M.W. JAROSIK*

Institute of Physics, Częstochowa University of Technology, Al. Armii Krajowej 19, 42-200 Częstochowa, Poland

The detailed study of the selected thermodynamic properties of the superconducting phase in the molecular hydrogen under the pressure at 428 GPa has been presented. For the increasing value of the Coulomb pseudopotential $\mu^* \in (0.08, 0.15)$, the following results have been obtained: (i) the critical temperature decreases from 179 K to 141 K, (ii) the ratio $R_1 \equiv 2\Delta(0)/k_B T_C$ differs noticeably from the BCS value: $R_1 \in (4.71, 3.60)$; (iii) the electron effective mass is large and grows slightly together with the temperature ($[m_e^*/m_e]_{\max} = 2.2$ for $T = T_C$).

PACS: 74.20.Fg, 74.25.Bt, 74.62.Fj

1. Introduction

At low temperature, hydrogen exhibits the nontrivial structural behavior under the pressure p [1, 2]. Below 110 GPa the hexagonal-closed-packed lattice with freely rotating molecules is stable (phase I). At higher pressures, up to 150 GPa, the broken symmetry phase has been observed (phase II). In the pressure range of 150–350 GPa the so called phase III exists. The experimental measurements have proved, that the all listed phases do not demonstrate the metallic properties. In the pressure range from ≈ 400 GPa to ≈ 500 GPa, the theoretical studies predict the existence of the molecular metallic phase (the *Cmca* crystal structure) [3–5]. Above ≈ 500 GPa, the molecular metallic phase transforms to the Cs-IV monatomic phase [3–6]. This phase is stable at least up to 802 GPa [7]. For the extremely high value of the pressure (2000 GPa) Maksimov and Savrasov have proposed the simple *fcc* structure [8].

The molecular and monatomic metallic form of the hydrogen can be the superconductor with the high critical temperature T_C [9]. In particular, the calculated values of the critical temperature have been presented in the Table. We notice that T_C has usually been obtained by using the McMillan formula [14], which represents the weak coupling limit of the more elaborate Eliashberg approach [15]. However, in the case of the metallic hydrogen the electron–phonon interaction is strong, hence the McMillan expression is inappropriate.

For this reason, we have calculated the critical temperature with the help of the Eliashberg equations. We have considered the case $p = 428$ GPa (the value of p close to the metallization pressure). Additionally, we have studied precisely the properties of the order parameter and the electron effective mass.

In the paper we have taken into consideration the Eliashberg set in the mixed representation [16]. This approach allows one to obtain the stable solutions on

the real axis, since the analysis does not involve any principal-part integrals with singular integrands.

TABLE

The critical temperature for the selected values of the pressure; μ^* denotes the Coulomb pseudopotential.

p [GPa]	T_C [K]	μ^*	Structure	Ref.
400	130–230 ^a	0.1	<i>sh, dsh, 9R^b</i>	[10]
414	84	–	<i>Cmca</i>	[11]
428	162 ^a	0.1	<i>Cmca</i>	[12]
450	242 ^c	–	<i>Cmca</i>	[11]
480	284 (266) ^a	0.1 (0.13)	Cs-IV	[7]
539	291 (272) ^a	0.1 (0.13)	Cs-IV	[7]
608	291 (271) ^a	0.1 (0.13)	Cs-IV	[7]
802	282 (260) ^a	0.1 (0.13)	Cs-IV	[7]
2000	≈ 600	–	<i>fcc</i>	[8]
2000	(631, 413) ^d	(0.1, 0.5)	<i>fcc</i>	[13]

^aThe McMillan formula [14]. ^bProbably unstable.

^cThe three-band model. ^dThe exact solution of the Eliashberg equations [15].

2. The Eliashberg equations

The Eliashberg equations in the mixed representation have been written in the following form [16]:

$$\begin{aligned}
 \phi(\omega) = & \frac{\pi}{\beta} \sum_{m=-M}^M \frac{(\lambda(\omega - i\omega_m) - \mu^*(\omega_m))}{\sqrt{\omega_m^2 Z_m^2 + \phi_m^2}} \phi_m \\
 & + i\pi \int_0^{+\infty} d\omega' \alpha^2 F(\omega') \left((N(\omega') + f(\omega' - \omega)) \right. \\
 & \times K(\omega, -\omega') \phi(\omega - \omega') \Big) \\
 & + i\pi \int_0^{+\infty} d\omega' \alpha^2 F(\omega') \left((N(\omega') + f(\omega' + \omega)) \right. \\
 & \times K(\omega, \omega') \phi(\omega + \omega') \Big), \quad (1)
 \end{aligned}$$

and

* e-mail: jarosikmw@wip.pcz.pl

$$\begin{aligned}
Z(\omega) = & 1 + \frac{i\pi}{\omega\beta} \sum_{m=-M}^M \frac{\lambda(\omega - i\omega_m)\omega_m}{\sqrt{\omega_m^2 Z_m^2 + \phi_m^2}} Z_m \\
& + \frac{i\pi}{\omega} \int_0^{+\infty} d\omega' \alpha^2 F(\omega') \left((N(\omega') + f(\omega' - \omega)) \right. \\
& \times K(\omega, -\omega') (\omega - \omega') Z(\omega - \omega') \\
& \left. + \frac{i\pi}{\omega} \int_0^{+\infty} d\omega' \alpha^2 F(\omega') \left((N(\omega') + f(\omega' + \omega)) \right) \right. \\
& \times K(\omega, \omega') (\omega + \omega') Z(\omega + \omega') \Big), \quad (2)
\end{aligned}$$

where:

$$\begin{aligned}
K(\omega, \omega') & \\
& \equiv \frac{1}{\sqrt{(\omega + \omega')^2 Z^2(\omega + \omega') - \phi^2(\omega + \omega')}}. \quad (3)
\end{aligned}$$

The Eliashberg set gives the following solutions on the real axis: the order parameter function $\phi(\omega)$ and the wave function renormalization factor $Z(\omega)$. The order parameter is defined by the expression: $\Delta(\omega) \equiv \phi(\omega)/Z(\omega)$. On the other hand, the imaginary axis functions ($\phi_m \equiv \phi(i\omega_m)$ and $Z_m \equiv Z(i\omega_m)$) should be calculated by using the equations:

$$\phi_n = \frac{\pi}{\beta} \sum_{m=-M}^M \frac{\lambda(i\omega_n - i\omega_m) - \mu^*(\omega_m)}{\sqrt{\omega_m^2 Z_m^2 + \phi_m^2}} \phi_m, \quad (4)$$

and

$$Z_n = 1 + \frac{1}{\omega_n} \frac{\pi}{\beta} \sum_{m=-M}^M \frac{\lambda(i\omega_n - i\omega_m)}{\sqrt{\omega_m^2 Z_m^2 + \phi_m^2}} \omega_m Z_m, \quad (5)$$

where the Matsubara energy is given by: $\omega_m \equiv (\pi/\beta)(2m-1)$ and $\beta \equiv (k_B T)^{-1}$; k_B is the Boltzmann constant.

The pairing kernel for the electron-phonon interaction has the form:

$$\lambda(z) \equiv 2 \int_0^{\Omega_{\max}} d\Omega \frac{\Omega}{\Omega^2 - z^2} \alpha^2 F(\Omega). \quad (6)$$

The Eliashberg function for the molecular hydrogen ($\alpha^2 F(\Omega)$) has been calculated in [12]. The maximum phonon energy (Ω_{\max}) is equal to 508.1 meV.

The function $\mu^*(\omega_m) \equiv \mu^* \theta(\omega_c - |\omega_m|)$ describes the Coulomb repulsion between electrons; μ^* denotes the Coulomb pseudopotential, θ is the Heaviside unit function and ω_c represents the energy cut-off ($\omega_c = 3\Omega_{\max}$). For the molecular hydrogen we assume: $\mu^* \in \langle 0.08, 0.15 \rangle$.

The symbols $N(\omega)$ and $f(\omega)$ denote the Bose and Fermi functions respectively.

The Eliashberg equations have been solved for 1601 Matsubara frequencies ($M = 800$) by using the numerical method presented in the papers [17]. In the considered case, the functions $\phi(\omega)$ and $Z(\omega)$ are stable for $T \geq 11.6$ K.

3. Results

In Fig. 1 we have presented the dependence of the critical temperature on the value of the Coulomb pseudop-

tential. The exact numerical solutions of the Eliashberg equations have been represented by the black circles. The dashed and dotted lines represent the calculation of the critical temperature by using Allen-Dynes formula [18] and the McMillan expression respectively. It is easy to see, that McMillan formula lowers much T_C in the whole range of the Coulomb pseudopotential's values, whereas the Allen-Dynes expression predicts correctly the critical temperature only for very low values of μ^* . For this reason we have modified the classical Allen-Dynes expression in order to obtain the analytical formula, which reproduces the Eliashberg results exactly (the solid line in Fig. 1). In particular, we have fitted the selected

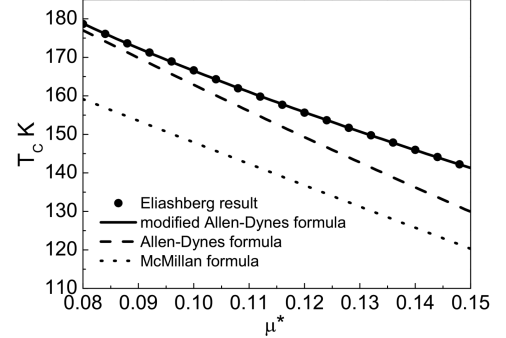


Fig. 1. The critical temperature as a function of the Coulomb pseudopotential.

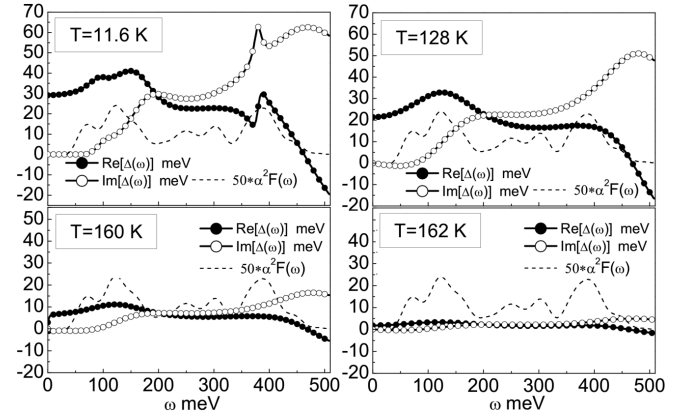


Fig. 2. The real and imaginary part of the order parameter on the real axis for the selected temperatures. The rescaled Eliashberg function is also plotted.

parameters in the Allen-Dynes expression (A_1 and A_2) with the help of 250 numerical values of $T_C(\mu^*)$. The final result takes the form:

$$k_B T_C = f_1 f_2 \frac{\omega_{\ln}}{1.2} \exp\left(\frac{-1.04(1+\lambda)}{\lambda - \mu^*(1+0.62\lambda)}\right), \quad (7)$$

where:

$$f_1 \equiv \left(1 + \left(\frac{\lambda}{A_1}\right)^{\frac{2}{3}}\right)^{\frac{1}{3}} \text{ and}$$

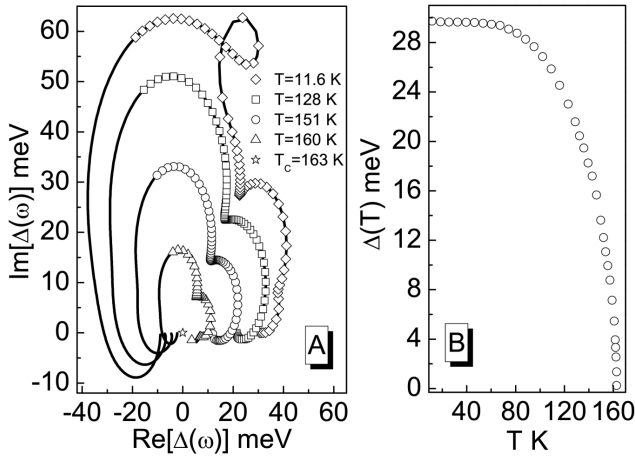


Fig. 3. (a) The order parameter on the complex plane for the selected values of the temperature. The lines with symbols represent the solutions for $\omega \in \langle 0, \Omega_{\max} \rangle$, whereas the regular lines correspond to the solutions for $\omega \in (\Omega_{\max}, \omega_c)$. (b) The temperature dependence of the order parameter. In the both cases we assume $\mu^* = 0.1$.

$$f_2 \equiv 1 + \frac{\left(\frac{\sqrt{\omega_2}}{\omega_{\text{In}}} - 1\right) \lambda^2}{\lambda^2 + A_2^2}. \quad (8)$$

Additionally:

$$A_1 \equiv 3.64 - 12.92\mu^* \text{ and}$$

$$A_2 \equiv \frac{\sqrt{\omega_2}}{\omega_{\text{In}}} (1.39 - 59.74\mu^*). \quad (9)$$

The parameters: λ , $\sqrt{\omega_2}$ and ω_{In} are equal to: 1.2 meV, 207.5 meV and 141.9 meV, respectively.

In Fig. 2 we have shown the order parameter on the real axis for the selected temperatures, and $\mu^* = 0.1$; the Eliashberg function is also plotted. On the basis of the presented results one can state, that both the real and imaginary part of the function $\Delta(\omega)$ is plainly correlated with the shape of the electron–phonon interaction. This effect is especially clearly visible for the low values of the temperature. The full form of the order parameter on the complex plane has been presented in Fig. 3a. We have stated, that the $\Delta(\omega)$ values form the distorted spirals which shrink with the growth of the temperature. Basing on Fig. 3a it is also possible to notice, that the effective electron–electron interaction is attractive ($\text{Re}(\Delta(\omega)) > 0$) in the range of the frequencies from zero to $\approx 0.9\Omega_{\max}$.

Taking into consideration the equation: $\Delta(T) = \text{Re}(\Delta(\omega = \Delta(T)))$ we have calculated the dependence of the order parameter on the temperature (see Fig. 3b). Next, the value of the ratio $R_1 \equiv \frac{2\Delta(0)}{k_B T_C}$ can be obtained, where $\Delta(0)$ denotes the value of the order parameter close to the zero temperature and $\Delta(0) \simeq \Delta(T = 11.6\text{K})$. In Fig. 4 we have presented the possible values of R_1 for $\mu^* \in \langle 0.08, 0.15 \rangle$. It is easy to see that in the whole range of the considered values of the Coulomb pseudopotential, the ratio R_1 differs essentially

from the BCS prediction; $[R_1]_{\text{BCS}} = 3.53$ [19]. Additionally, in the inset in Fig. 4 we have shown the dependence of $\Delta(0)$ on μ^* .

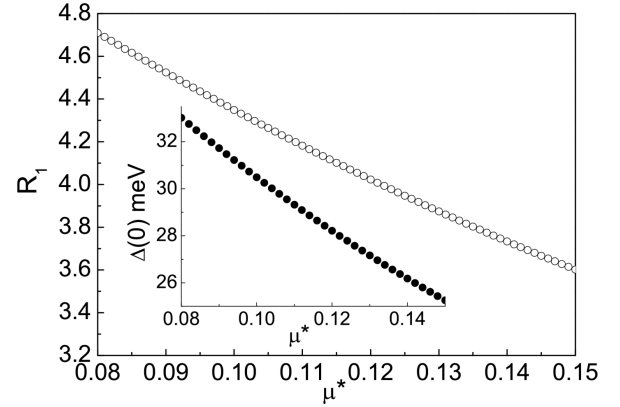


Fig. 4. The ratio R_1 as a function of the Coulomb pseudopotential. The inset shows the open form of $\Delta(0)$.

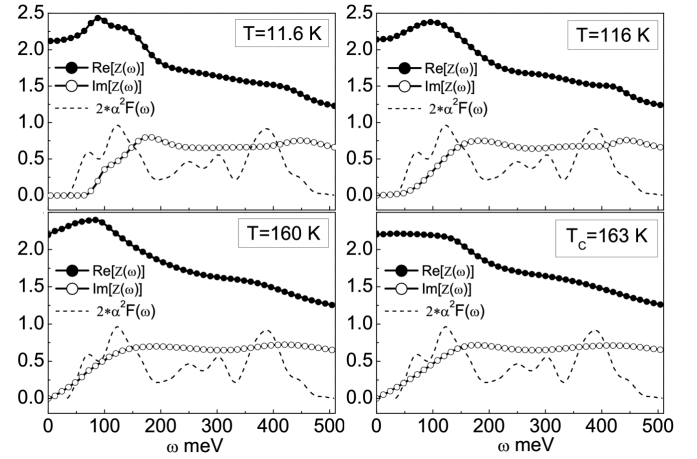


Fig. 5. The real and imaginary part of the wave function renormalization factor on the real axis for the selected temperatures. The rescaled Eliashberg function is also plotted.

The second solution of the Eliashberg equations on the real axis has been plotted in Fig. 5 ($\mu^* = 0.1$). The obtained results prove that the function $Z(\omega)$ also clearly senses the structure of the electron–phonon interaction. The shape of the wave function renormalization factor on the complex plane has been presented in Fig. 6. We see, that in contrast to the order parameter, the function $Z(\omega)$ weakly depends on the temperature.

In the framework of the Eliashberg formalism, on the basis of the wave function renormalization factor, the temperature dependence of the electron effective mass (m_e^*) can be calculated. In particular: $m_e^*/m_e = \text{Re}[Z(0)]$, where the symbol m_e denotes the bare electron mass. The values of the ratio m_e^*/m_e have been pre-

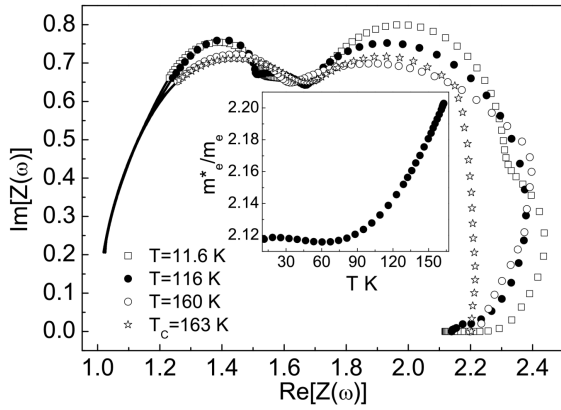


Fig. 6. The wave function renormalization factor on the complex plane ($\mu^* = 0.1$). The lines with symbols represent the solutions for $\omega \in \langle 0, \Omega_{\max} \rangle$, whereas the regular lines correspond to the solutions for $\omega \in \langle \Omega_{\max}, \omega_c \rangle$. The inset shows the ratio m_e^*/m_e as a function of the temperature.

sented in the Fig's. 6 inset. According to the presented data, it is easy to spot, that m_e^* is high in the full range of the considered temperatures and $[m_e^*/m_e]_{\max} = 2.2$ for $T = T_C$. We notice that at the critical temperature, the electron effective mass is independent of μ^* and $[m_e^*/m_e]_{\max} = 1 + \lambda$.

4. Summary

We have calculated the selected thermodynamic properties of the superconducting state in the molecular hydrogen ($p = 428$ GPa). The numerical analysis has been conducted in the framework of the one-band Eliashberg formalism for the wide range of the Coulomb pseudopotential's values: $\mu^* \in \langle 0.08, 0.15 \rangle$. We have proved, that the critical temperature is high even for large values of μ^* ($[T_C]_{\min} = 141$ K). Next, it has been shown, that the superconducting phase is characterized by high value of the dimensionless ratio R_1 , which differs from the BCS result; $R_1 \in \langle 4.71, 3.60 \rangle$. Finally, we have observed that the electron-phonon interaction strongly enhances the effective electron mass for the temperatures from zero to T_C . In particular, the maximum of m_e^* is equal to $2.2m_e$ for $T = T_C$.

In the future we will analyze the superconducting state in the molecular hydrogen in the framework of the three-gap Eliashberg model. It will be done in order to discuss the effect of the multi-band anisotropy [11].

Acknowledgments

The authors wish to thank K. Dziłiński for providing excellent working conditions and the financial support; A.P. Durajski and D. Szczęśniak for the productive scientific discussion that improved the quality of the presented paper. Some computational resources have been provided by the RSC Computing Center.

References

- [1] C. Narayana, H. Luo, J. Orloff, A.L. Ruoff, *Nature* **393**, 46 (1998).
- [2] P. Loubeyre, F. Occelli, R. LeToullec, *Nature* **416**, 613 (2002).
- [3] K. Johnson, N.W. Ashcroft, *Nature* **403**, 632 (2000).
- [4] M. Stadelé, R.M. Martin, *Phys. Rev. Lett.* **84**, 6070 (2000).
- [5] C.J. Pickard, R. Needs, *Nat. Phys.* **3**, 473 (2007).
- [6] V. Natoli, R.M. Martin, D.M. Ceperley, *Phys. Rev. Lett.* **70**, 1952 (1993).
- [7] Y. Yan, J. Gongb, Y. Liu, *Phys. Lett. A* **375**, 1264 (2011).
- [8] E.G. Maksimov, D.Y. Savrasov, *Solid State Commun.* **119**, 569 (2001).
- [9] N.W. Ashcroft, *Phys. Rev. Lett.* **21**, 1748 (1968).
- [10] T.W. Barbee, M.L. Cohen, *Phys. Rev. B* **143**, 5269 (1991).
- [11] P. Cudazzo, G. Profeta, A. Sanna, A. Floris, A. Continenza, S. Massidda, E.K.U. Gross, *Phys. Rev. Lett.* **100**, 257001 (2008).
- [12] L. Zhang, Y. Niu, Q. Li, T. Cui, Y. Wang, Y. Ma, Z. He, G. Zou, *Solid State Commun.* **141**, 610 (2007).
- [13] R. Szczęśniak, M.W. Jarosik, *Solid State Commun.* **149**, 2053 (2009).
- [14] W.L. McMillan, *Phys. Rev.* **167**, 331 (1968).
- [15] G.M. Eliashberg, *Soviet. Phys. JETP* **11**, 696 (1960).
- [16] F. Marsiglio, M. Schossmann, J.P. Carbotte, *Phys. Rev. B* **37**, 4965 (1988).
- [17] R. Szczęśniak, *Solid State Commun.* **138**, 347 (2006); R. Szczęśniak, *Physica Status Solidi (b)* **244**, 2538 (2007); R. Szczęśniak, M.W. Jarosik, D. Szczęśniak, *Physica B* **405**, 4897 (2010); M.W. Jarosik, R. Szczęśniak, D. Szczęśniak, *Acta Phys. Pol. A* **118**, 1031 (2010).
- [18] P.B. Allen, R.C. Dynes, *Phys. Rev. B* **12**, 905 (1975).
- [19] J. Bardeen, L.N. Cooper, J.R. Schrieffer, *Phys. Rev.* **108**, 1175 (1957).